326 | https://doi.org/10.3311/PPme.17848
Creative Commons Attribution

Periodica Polytechnica Mechanical Engineering, 65(4), pp. 326–336, 2021

An Experimental Study on the Force Coefficient and the Discharge Coefficient of a Safety Valve in Air-water Mixture Flow

Mhd Ghaith Burhani[1], Csaba Hős[1*]

[1] Department of Hydrodynamic Systems, Faculty of Mechanical Engineering, Budapest University of Technology and Economics, Műegyetem rkp. 3, 1111 Budapest, Hungary
[*] Corresponding author, e-mail: cshos@hds.bme.hu

Received: 13 January 2021, Accepted: 11 May 2021, Published online: 21 September 2021

Abstract

Due to the low number of experimental investigations on the sizing of safety valves in multiphase flow, a novel set of measurement data of an air-water mixture is reported. This paper presents an experimental study on three different geometries of safety valves, a poppet valve with jet angle $\theta = 120°$, and two-disc valves with deflection angles $\theta = 0°$ and $\theta = 90°$, respectively. Our test rig comprises a pipeline with 42.5 mm inner diameter, spray nozzles to supply the added water quality (water mass fraction) to the pressurized airflow up to 40 % mass fraction and an inlet pressure up to 6.6 bar(g). The time histories of force, valve lift, and pressures were recorded. We present correlation data for the force coefficient and the discharge coefficient. The widely used omega technique for the Homogenous Equilibrium Model (HEM) is employed to predict the theoretical mass flux. The results show that the poppet valve experiences less momentum force and lower mass flow rates compared to disc valves, while the disc valve with deflection angle $\theta = 90°$ presents the highest discharged flow rates among the tested geometries. Our most important finding is that up to 60 % relative valve lift and 40 % mass fraction, neither the force nor the discharge coefficient changes significantly compared to the pure-air case. Finally, we propose a new correlation with a single equation for the resultant force and the discharge coefficient as a function of the relative valve lift for all tested water mass fractions.

Keywords

force coefficient, air-water mixture, discharge coefficient, safety valve, experimental

1 Introduction

A safety valve is a crucial part of any hydraulic power transmission system, chemical plant, petrochemical facility, industrial gas and liquid service or nuclear power station. The presence of these devices is vital to provide overpressure protection and to keep the pressure beneath the Maximum Allowable Working Pressure (MAWP) at a designated temperature under normal operating conditions, see [1].

Despite the widely available application range of safety valves [2–4], their sizing in the case of multi-phase is still ambiguous matter and hard to predict because of the complexity of multi-phase flows nature, as stated, e.g., in [5]. The unpredictable fluid mixture flashing (evaporation) due to the sudden pressure drop through the valve causes a phase change which in turn may result in valve chattering, leading to insufficient venting capacity and eventually to the catastrophic rupture of the system (undersizing and oversizing of safety valves), see, e.g. [6–8]. The safety valve, which is a single degree of freedom oscillator [9–11], shows a high complex dynamical behaviour as mentioned in [12] which demands more investigations and experimental work, notably to define the flow force behavior and the characteristics of discharging in case of emergency scenarios.

To deal with and to understand the dynamical stability of a safety valve successfully, it is essential to capture the actual mass flux of the fluid through it and to model the generated force on the valve disc as well. Several approaches have been applied for the latter purpose, including single-phase and two-phase cases by either using the straightforward concept of "effective area" proposed by Hős et al. [13], or by utilizing the deflection angle technique, which introduced in Darby works, see for details [14, 15].

Cite this article as: Burhani, M. G., Hős, C. "An Experimental Study on the Force Coefficient and the Discharge Coefficient of a Safety Valve in Air-water Mixture Flow", Periodica Polytechnica Mechanical Engineering, 65(4), pp. 326–336, 2021. https://doi.org/10.3311/PPme.17848

This paper discusses the effect of adding constant water mass fractions to a pressurized airflow (i.e. frozen mixture) experimentally. The research covers three different geometries of safety valves (poppet and disc valves), seeking a prediction of a single modelling equation for both the dimensionless force (effective area) and the discharge coefficient terms, which is valid and applicable for all tested water qualities under certain conditions. Our model assumes a constant mass fraction that can be applied for bubbly flows or in the case of the humid airflow, where no matter how the volume fraction of the air changes due to the pressure changes, the mass fraction stays constant, see, e.g., [16–19].

Employing DIER's omega technique provides the evaluation of the theoretical mass flux of the frozen flow (i.e. non-flashing) and later allows the eliciting of the discharge coefficients after measuring the actual mass flow rate experimentally. This technique is prevalent in estimating the mass flow rates for both flashing (e.g. steam-water, and saturated liquid) as stated in [20, 21], and non-flashing flow (i.e. air-cold water); see for details [22, 23]. Leung (omega method), in his paper assumes thermodynamic and mechanical equilibrium; that is, the isentropic path of the flow and that both phases travel with the same velocity (no-slip). Moreover, the omega technique is an applicable and valid approach in the case of subcritical flow and the critical (choked) flow, where it only requires the fluid properties at the stagnation (inlet) conditions. Regardless of the disadvantages and the limitations of omega methods in portending of the theoretical mass flow rate through the short nozzles (valve) near the critical points as mentioned in [24], its simplicity and flexibility still show promising results and an acceptable competency among the rest of complex techniques HNE, TPHEM, and HDI (more accurate), see for details [25].

This paper involves the following sections. Section 2 contains the literature review. Then, safety valve geometries description with their governing equations are introduced in Section 3. Sections 4 presents the test facility and the procedure of the measurement. Next, Section 5 includes the results and the discussion regarding the effective area and discharge coefficient. Finally, Section 6 reveals the conclusion and the summary.

2 Literature review

The flow protection and avoidance of reaching oversizing or undersizing cases are the primary goals of the optimal sizing of the safety valves (e.g. Pressure Relief Valve) when the pressure or the temperature exceeds the preset limits. A safety valve might show unstable dynamical performance (i.e. the insufficient capacity of blowdown) during the urgent scenarios of relieving the working medium (overpressure) from either a reservoir or a boiler. Hence, the instability resulting in a hydraulic plant system failure (a shutdown or a rupture of pipeline and pressure vessel) and the demand for a full dynamic analysis of the safety valve behavior (especially in the case of multi-phase) forms a necessity to identify the mass flow rates and the applied forces on the valve disc correctly. The two-phase flow requires an additional degree of freedom compared with the single-phase flow, that is, the gas or the liquid mass fraction. This fluid quality imposes a more profound knowledge of thermodynamics processes, which make the procedure of predicting the characteristics of flow laborious. In the next paragraph, we point out some of CFD modellings and previous experimental works of safety valves under a multi-phase condition with emphasizing on the air-water mixture empirical researches that are to the authors' knowledge and interests.

Burhani and Hős [26] discussed the flow behavior of a poppet valve (only) experimentally in the case of non-flashing flow (i.e. frozen flow) under the assumption of the steady-state condition and a studied interval of water injection up to 30.8 % to a pressurized airflow. The empirical results show that the effective area (fluid force) tends to increase as the injected water ratio increases. The trend of the effective area of all water ratios starts from unity and slightly increasing correspond to a relative valve lift of 0.2 before it decreases again up to 0.8 of the relative opening position. On the other hand, the higher the water mass fraction is, the higher the resultant discharge coefficient becomes, where the tendencies of the characteristics curve of the discharge coefficients of all water mass fractions show consistent performance and decrease with the increase of the relative valve lift. Furthermore, beyond 0.6 % relative displacement, the values of these coefficients are constant corresponding to each water ratio. The present work is a natural continuation of this measurement, and in this paper, we present improved measurement results on the poppet valve, plus novel results for the disc valve geometries.

Burhani and Hős in [27] reported a numerical study in the case of frozen flow (air to water mixture) through a Pressure Relief Valve (PRV) on the dynamic behavior by applying DIER's omega technique to estimate the mass flux against different gas qualities. The impulse force of three geometries of PRVs analysis was recorded for

incompressible and compressible flows, and an estimation of the opening time of PRV with the help of Matlab code was conducted. The fluid force results are in reasonable agreement with the corresponding literature: the increase of the fluid mass fraction does not vary the overall force on the valve disc significantly. Furthermore, the estimated opening time drastically changes versus a trivial gas mass fraction which results in a fast response of the valve (pops up) within a few tenth of seconds.

Scuro et al. [28] investigated a three-dimensional numerical study on the flow dynamics of a Direct-Operated Safety Relief Valve (DOSRV) by employing ANSYS-CFX commercial code for several openings and upstream pressures under a steady-state condition. The obtained simulation results of the disc force and the discharge coefficients of dry saturated steam revised by IAPWS-IF97 show a consistent behaviour for opening positions less than 12 mm and outstanding performance when compared with the ASME standard. On the other hand, the averaged normal force is about 19 % lower than the theoretical force of the ASME standard. Additionally, validation of a transonic of airflow was performed through a converging-diverging diffuser, and it shows an acceptable agreement with the provided experimental data.

Dempster and Alshaikh [29] studied the flow and force characteristics of air-water mixture flow experimentally through a Safety Relief Valve (SRV) which is used extensively in the refrigeration industries. The investigated range of pressure is 5–14 bar(a), and the liquid mass fractions varying from 0 % (pure gas) up to 79 %, and the experiment was repeated for different opening positions. The authors concluded that the injected water quality affects both the flow rates and the disc forces with a more prominent influence on the mass flux of the mixture. The airflow rate is reduced by more than 50 % at 5 mm valve lift (maximum lift) for 0.79 of water quality. Simultaneously, the force change is relatively small for the same applied liquid mass fraction as the force reduction is 10 % less than the force of the pure gas (air) flow corresponds to a 5 mm opening position.

Arnulfo et al. [30] reproduced an experimental data set of air-water mixtures flow and steam-water flow to evaluate the discharge coefficients of choked flow in a safety valve. The authors employed several approaches of mass flow rates prediction through the ideal nozzle such as Omega, HDI, HNDI, HFM Starkman, and HFM Nastoll, which are proposed by Lenzing, Leung, and Darby. They concluded that in the case of flashing flows, the applying of the multiplication of the Lenzing discharge coefficient with the one obtained by HNDI in the critical flow case could show promising results. On the other side, for non-flashing flows (e.g. air-water mixture), Leung/Darby formulation with the omega method is more adequate for estimating the flow rate than the rest of the theories.

Dempster and Elmayyah [31] presented the prediction of discharge flow in the case of non-flashing through a Safety Relief Valve by using a CFD tool. They compared their model against an experimental work of Safety Relief Valve that used in the industrial refrigeration within pressure range 6–15 bar(g) and air mass qualities varying from 0.1 up to 1 when the discharging occur near the atmospheric conditions at fully opening position of the safety valve. Additionally, the mixture CFD model results have been compared with the Homogenous Equilibrium Model (HEM). The consequences show that the CFD model and the HEM omega model have an excellent matching within the same mass fraction interval, and the CFD and HEM models give an adequate critical mass flow rate prediction of two-phase non-flashing flow with a liquid quality up to 0.4. On the other hand, this investigation recorded an error of roughly 15 % for a larger liquid mass fraction (up to 0.9).

Another experimental study of a Safety Relief Valve in the case of a critical flow of air-water mixture is conducted on an industrial refrigeration valve with a discharging towards the atmosphere and for different valve lifts [32]. The operating pressure range of 6–15 bar(g), with water mass fraction varying between (0) and (0.7), and air mass flow rates range of (0.01–0.05 kg/s). The experimental results were compared with a CFD model, while the outcome of the CFD model was examined versus the ideal nozzles mass flux models, that is, DIER's ω method and HNE-DS, which are adopted by the ISO standard. Consequently, the mixture CFD model is consistent with the experimental results for large valve opening positions at a low water mass fraction (0.11) with a discrepancy of 0.5 %. However, the accuracy of the flow rate estimation reduces when the water quality increases: the error was 9 % at 55 % water quality. In addition, for small valve lifts (0.25–1 mm), the deviation of the predicted results from the experiments grows up to around 16 %.

Accordingly, and due to insufficient experimental investigations for safety valves in the case of the two-phase flow (frozen flow), our work aims to present and add a novel set of measurement data using mixture flow (i.e., air-cold water mixture). Hence, another contribution

can be added to the existing body of experiments done in previous works and researches. This paper reports the effective area (force coefficient) and the discharge coefficients for three safety valve geometries utilized in industries for various purposes (e.g., gas service, oil service, hydraulic transmission power plant). This empirical work is conducting within a wide range of air-water mixture flow up to 60 % relative valve lift and 40 % water mass fraction. Consequently, the resultant proposed is a single correlation for both the momentum force and discharged flow rates, contributing to optimizing and sizing the safety valves in various industrial areas and applications.

3 ISO description of a safety valve

Safety valves are available in a wide range of size to meet and satisfy the performance criteria of different applications demanded by various industries. The International Organization for Standardization (ISO) defines several types of safety valves such as direct-loaded safety valves, assisted safety valves, and pilot-operated safety valves. These valves commonly consist of the valve body connected to the moving parts (i.e. disc and disc holder) and the bonnet, which is mounted to the valve body by either welding or thread. Inside the bonnet, there is a spindle, a spring, and an adjustment screw, allowing the adjustment of the spring compression and hence the set pressure; see for more details [1, 33].

When the pressure inside the system reaches the maximum allowed pressure, the valve pops (quickly opens) and vents the overpressure out to the discharge side keeping and protecting the mechanical assembly from rupture or explosion. Once the system pressure decreases below the reseat pressure, the valve tends to closes. The difference between the set pressure and reseating pressure expressed as a percentage of set pressure is the so-called blowdown which is a crucial term in predicting the opening and closing cycles [7, 12].

3.1 Safety valve geometries

Our investigation of the frozen flow characteristics through the safety valves involves three different typical geometries with varying angles of deflection, as shown in Fig. 1. Fig. 1 (a) shows a geometry employed commonly in the hydraulic power transmission systems with a jet angle larger than 90 degrees. The conical design results in a decreasing overall fluid force as the valve lift increases. On the other hand, Fig. 1 (b) and (c) depicts disc valves with jet angles θ = 0°, and θ = 90°, respectively. These types are widely employed in the oil and gas industry and piston compressors. In contrast to the poppet valve, the

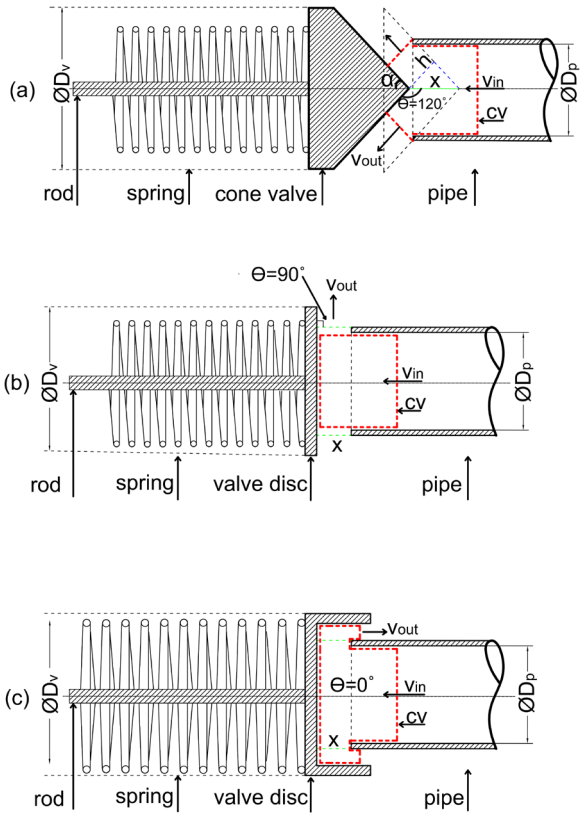

Fig. 1 Schematic of the analyzed safety valve geometries. (a) poppet (conical) valve with jet angle $\theta = 120°$, (b) and (c): disc valves with jet angles $\theta = 90°$, $\theta = 0°$ respectively. The red dashed line stands for the control volume of the confined water flow.

overall force of the disc valves is larger than the one of the cone valve (poppet) because of the positive contribution provided by the momentum force. In addition, disc valves grant a higher mass flow rate compared with the cone valve design (see Figs. 5 and 6 of [27]).

3.2 Mathematical formulation

In what follows, we present the governing equations of the fluid flow through the safety valve covering the impulse force, the equation of motion of a single-DOF oscillator, and the theoretical mass flux equation by employing DIER's omega technique.

When the valve opens, the generated fluid force on the disc (reaction of fluid force) can be expressed by applying the momentum theory [34] on a specific control volume (see the red dashed lines in Fig. 1). This theory claims that the sum of all applied forces on the chosen control volume equals the temporal rate of momentum change through the control surface, that is:

$$F\left(x, p_0, p_b\right) = \frac{\partial}{\partial t}\int_{\Omega} \rho v \mathrm{d}V + \int_{\partial\Omega} \rho v \left(v \mathrm{d}A\right) + \int_{\partial\Omega} \rho \mathrm{d}A. \qquad (1)$$

Equation (1) shows the fluid force, which is typically a function of valve lift x, upstream pressure p_0 and downstream pressure (backpressure) p_b, which might be different from the atmospheric pressure, but, in this study we assume it to be constant and equals to the atmospheric pressure ($p_b = p_a$). This is a typical case when there is no outlet collector piping and the valve vents directly to the atmosphere. Moreover, the first term on the right-hand side of Eq. (1) stands for the unsteady part resulting from the change of the deformable volume, while the second and the third terms refer to the momentum force and pressure force. The unsteady term can usually be neglected, see [9, 14, 26, 27]. Furthermore, the impulse and pressure forces should be evaluated on the boundary $\partial\Omega$ of the control volume, and Eq. (1) turns into two main forces, the pressure force and the impulse force at the inlet and outlet flow through the control volume:

$$\begin{aligned} F\left(x, p_0, p_b\right) &= F_{\text{pressure}} + \sum_{\text{out}} \dot{m} v_{\text{out}} + \sum_{\text{in}} \dot{m} v_{\text{in}} \\ &= A_v\left(p_0 - p_b\right) + \rho_{\text{out}} v_{\text{out}}^2 \cos\theta A_{\text{out}} + \rho_{\text{in}} v_{\text{in}}^2 A_{\text{in}}, \end{aligned} \tag{2}$$

where $\dot{m}$ is the mass flow rate, A_v stands for disc area of the valve, A_{in} is the inlet area and A_{out} denotes the outlet flow-through area. The ρ_{in}, ρ_{out}, v_{in} and v_{out} are the densities and velocities of the flow at the inlet and the outlet of the control volume, respectively. Finally, θ is the deflection angle (jet angle).

On the other hand, the overall fluid force (the left-hand side of Eq. (2)) combines three effects: pressure distribution, momentum change of fluid, and the wall shear distribution. This fluid force equals the overall dynamical state of the valve, that is

$$m\ddot{x} + k\dot{x} + s\left(x + x_0\right) = F\left(x, p_0, p_b\right), \tag{3}$$

where x, $\dot{x}$, $\ddot{x}$, x_0 denote the valve displacement, velocity, acceleration, and pre-tension of the spring. The k is the viscous damping coefficient, and s represents the spring stiffness coefficient.

We introduce a dimensionless quantity A_{eff} "effective area", which highlights the importance of the momentum force relative to the pressure force, and, after reformulating Eq. (2) we have

$$F\left(x, p_0, p_b\right) = A_{eff(x)} A_v\left(p_0 - p_b\right), \tag{4}$$

or

$$A_{eff}\left(x\right) = \frac{F\left(x, p_0, p_b\right)}{F_{\text{pressure}}}. \tag{5}$$

The pressure force $A_v(p_0 - p_b)$ represents the pressure difference between the upper surface and the lower surface of the valve disc. The pressure profile on the remaining surfaces of the disc is assumed to be uniformly distributed, and the axial component of the pressure force at the outer surfaces of the control volume is trivial; for details, see [26, 27].

Either Eq. (4) or Eq. (5) gives a direct and convenient way of estimating the overall fluid force as it requires only the upstream pressure, discharge pressure, and valve lift.

The theoretical mass flux through a safety valve (i.e. ideal short nozzle) can be estimated by utilizing the compressibility flow number (omega method), which assumes a well-mixed "pseudo-single" flow in the condition of thermal and mechanical equilibrium [21]. This approach can handle two-phase mixture flows and consists of two terms; the first reflects the compressibility of the two-phase mixture due to the existing vapour volume, and the second refers to the phase change due to the depressurization

$$\omega = \alpha_0 + \left(1 - \alpha_0\right)\omega_s, \tag{6}$$

where ω_s stands for the compressible flow number under a saturated condition (see for details [24]), while α_0 is the void fraction of the gas, given by

$$\alpha_0 = \frac{x_g}{x_g + \left(1 - x_g\right)\dfrac{\rho_g}{\rho_l}}, \tag{7}$$

where ρ_g and ρ_l are gas and liquid densities, respectively. The x_g is the gas quality (gas mass fraction) of the mixture given by

$$x_g = \dot{m}_g \big/ \left(\dot{m}_g + \dot{m}_l\right), \tag{8}$$

or, similarly, liquid mass fraction can be defined as

$$x_l = \dot{m}_l \big/ \left(\dot{m}_g + \dot{m}_l\right), \tag{9}$$

where $\dot{m}_l$ and $\dot{m}_g$ are the mass flow rates of the liquid and the gas, respectively. Obviously, the sum of the gas and liquid fractions gives unity.

On the other hand, the combination of the Bernoulli equation in the case of isentropic and frictionless flow and the two-phase Equation of State (EOS) can give the theoretical mass flux expression G, which can be expressed in the dimensionless style as (see [24] for details)

$$\frac{G}{\left(p_0 \rho_0\right)^{1/2}} = \frac{\left(-2\left(\omega \ln\eta + (\omega - 1)(1 - \eta)\right)\right)^{1/2}}{\omega\left(\dfrac{1}{\eta} - 1\right) + 1}, \tag{10}$$

with $\eta = \frac{p}{p_0}$ being the ratio of the upstream pressure and the downstream pressure. In case of p being lower than the critical pressure p_c, a choked flow state will occur, and the mass flux will reach its maximum value, that is

$$\frac{G_c}{(p_0\rho_0)^{1/2}} = \frac{\eta_c}{\sqrt{\omega}}. \quad (11)$$

The critical ratio η_c should be computed by solving the non-linear equation (Eq. (12)) w.r.t. the target ω value, hence

$$\eta_c^2 + (\omega^2 - 2\omega)(1-\eta_c)^2 + 2\omega^2 \ln\eta_c + 2\omega^2(1-\eta_c) = 0. \quad (12)$$

4 Experimental set-up and procedure

The experimental work has been carried out at the laboratory of the Department of Hydrodynamic Systems at the Budapest University of Technology and Economics by using three commercial safety valves; a poppet valve (conical valve) with 60 mm diameter, and two-disc valves with 50 mm and 60 mm diameters. For all geometries, under the condition of a frozen flow (i.e. air-water mixture), the flow performance and the flow forces on the valve disc of the three geometries have been tested for various injected ratios of water quality with different opening positions.

Figs. 2 and 3 depict the experimental facility and the schematic of the test rig. The main elements of the facility are

- a pressurized air tank,
- a pipeline with 145 cm length,
- a sonic nozzle with a 10 mm diameter throat,
- two liquid spray nozzles, located in the centerline of the pipe,
- a mechanism for positioning the valve body,
- a safety valve (target body),
- an inductive displacement sensor BAW0029,
- a force sensor KM300,
- two pressure taps (sensors P6A),
- two Bourdon pressure gauges,
- a water hose,
- a regulator and
- a support disc.

Fig. 2 shows the air reservoir with 900 litre volume, which supplies the pressurized airflow to the main pipeline of the test rig. The compressed air into the tank comes from a compressor with 160 m^3/h flow rate, 22 kW power, and 980 rpm revolution number. The attached sonic nozzle (orifice) with 10 mm throat diameter allows measuring the mass flow rate of the air, which varies within the range 0–0.12 kg/s. The upstream (inlet) pressure range 5.5–6.6 bar(g), and the temperature change of the air during the expansion via the sonic nozzle is neglected. Additionally, the inlet pressure can be controlled and

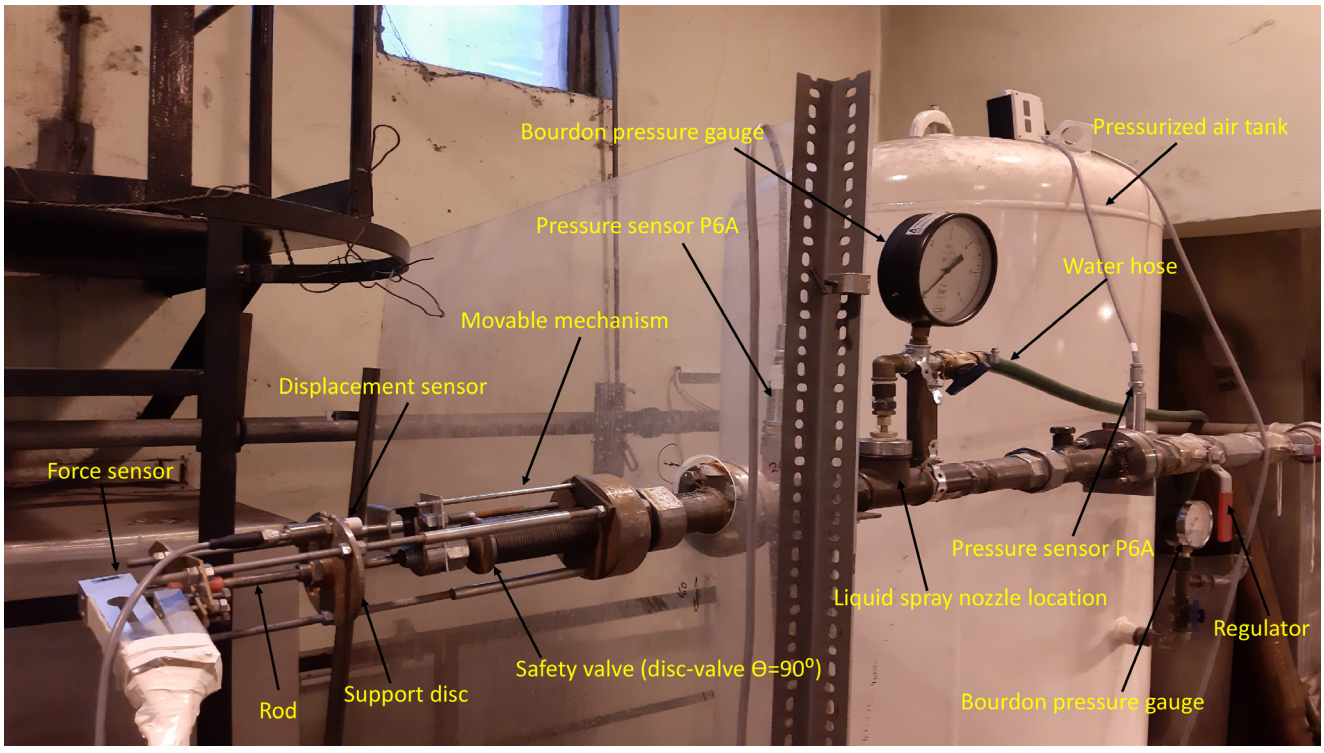

Fig. 2 Experimental facility of air-water mixture flow

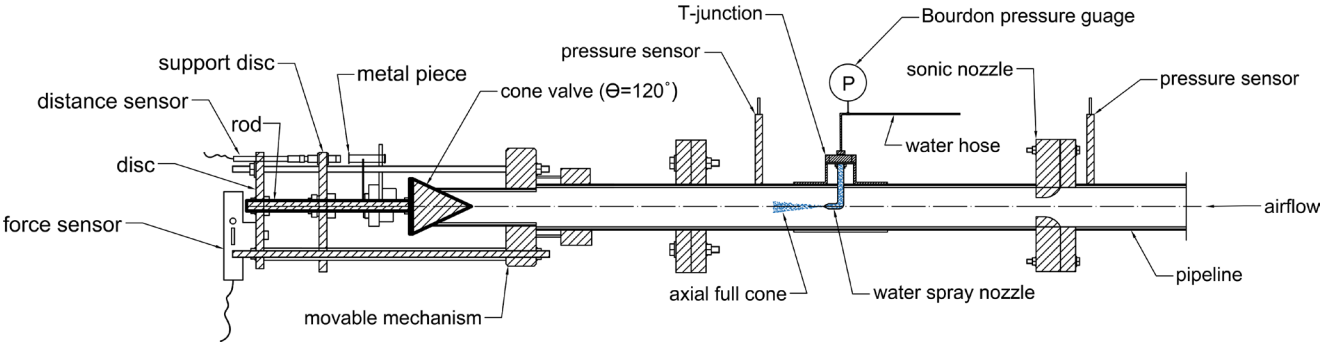

Fig. 3 Schematic of the experimental facility of frozen two-phase flow through safety valve (i.e. conical valve with $\theta = 120°$)

varied by a regulator set to full opening during the run of the measurements. The water spray nozzles have two different capacities, 1 and 5 litre/min (490.403 CA and 490.683 CC LECHLER), and they provide a full-cone profile of water with a 45-degree spray angle. The water quality varies between 0 % and 41 %, depending on the chosen pressure of the feedwater system. The first (small) spray nozzle gives small water ratios, while the second nozzle covers the rest of water mass fraction range.

Table 1 shows characteristics and properties of the utilized sensors in the experiment: two absolute pressure sensors (P6A), a force sensor (strain gauge KM300) and an inductive displacement sensor (BAW0029) were employed. The time histories are recorded and saved by means of the Catman software V3.5.1, connected to the 8-channel data acquisition hardware MX840A HBM.

Finally, a positioning mechanism holds the tested safety valve, the force transducer, and the displacement sensor completes the test rig. The mechanism can twist, allowing to set the desired opening position of the valve.

The varied parameters during the runs were the inlet water quality (water mass fraction) and the valve lift. The inlet pressure, the temperature of the tank, and the air mass flow rate were kept constant during the measurements:

- Water mass fractions provided by the first liquid spray nozzles with capacity 1 liter/min are: 6.5 %, 10 %, 13.25 %, 15.25 %, and 17.25 %.

Table 1 Characteristics and properties of sensors

Sensor	Code	Material	Weight	Working range	Accuracy
pressure	010 B P6A	Stainless steel 1.4305	200 g	0–10 bar(a)	±0.2 %
force	KM300	Aluminum alloy	300 g	0–1.2 KN	0.06 % F.S
distance	BAW-0029	Brass	600 g	4–16 mm	±0.3 mm

- Water mass fractions provided by the second spray nozzle with larger capacity 5 liter/min are: 27.3 %, 34 %, and 41 %.
- Valve opening positions varying (based on the applied pressure of the mixture) between 0.2 relative lift up to 0.6 relative lift, where the relative lift of the valve is defined as $\tilde{x} = 4x/D_p$, and x and D_p are the valve lift and the inner diameter of the pipeline respectively.
- The tank temperature t = 25 °C, inlet pressure p_0 = 6.6 bar(g), and air mass flow rate $\dot{m}_{\text{air}} = 0.12$ kg/s .

The measurements were proceeded by setting the injected water mass fraction with the help of the calibrated Bourdon pressure gauge (the upper Bourdon gauge, which is connected with the water source) as each pressure value of a Bourdon corresponds to specific water quality (e.g. 0.5 bar(g) provides 6.5 % of water quality). The next step was to open the regulator, which allows the airflow to travel through the pipeline and to mix with the water flow. Once the set pressure is built up in the pipeline, the valve opens, and the support disc retains and secures the concentric movement of the valve rod, and thus, the venting process occurs concentrically, see, Fig. 3. The time between the opening of the regulator and the closure is roughly 10 seconds, and within this span, the time histories of pressure, force, and displacement are recorded after cutting out an internal interval of a few seconds with stabilities pressure levels for post-processing purposes.

Ultimately, the load cell working principle of the force transducer during the run enforces to record valve lifts starting from approx. 2 mm (after cutting off the transient phase). At the same time, the displacement beneath this value could not be accomplished since while the valve moves to relieve the excessive pressure from the pipeline;

the valve rod simultaneously hits the edge of the sensor surface resulting in tensile strain; hence, an additional distance (approx. 1 mm) to be added to the valve lift.

5 Results and discussion

As it has been mentioned earlier, an essential step during the run for all tested water ratios is to record each of the pressures, force, and displacement time histories. The investigation includes the cases of the single-phase airflow and the frozen flow with eight different mass fraction of the water to be performed for three geometries of safety valves.

The water quality with the inlet pressure (upstream) and the air mass flow rates form the primary inputs of the measurements. At the same time, the outputs are the flow force on the valve disc and the actual mass flow rate of the mixture (water + air) through the safety valve. We plot the measured force data in terms of the "effective area" technique to highlight the importance of the impulse force by applying Eq. (5). On the other hand, employing Eq. (10) or Eq. (11) leads to predict the theoretical mass flow rate, which assists in extracting the discharge coefficient that provides a beneficial and practical background in sizing the safety valve in any industrial facility. However, the results for both effective area and discharge coefficient of safety valve geometries are represented with the experimental error (error bar) and are reported in Subsection 5.1 and Subsection 5.2 respectively.

5.1 Effective area

Fig. 4 depicts the momentum force impact on the disc valve in the case of poppet valve (see Fig. 1 (a)) for both the single-phase flow (i.e. airflow) and the mixture flow. The effective area for all tested water ratios shows the same trend, i.e., the decrease starting from 1 as the relative valve lift increases. The effective area of the cone valve geometry starts from a value near unity (purely pressure force) and decreases, reaching roughly 0.8 at relative lift $\tilde{x} = 0.55$. Note that this means decreasing overall fluid force with increasing valve opening, which is consistent with the theory. Moreover, as the water mass fraction increases, the effective area does not change significantly; hence, we conclude that the proposed effective area concept is valid for mass fraction up to 40 % and, more importantly, the measurement results with pure air can be used in the case of multiphase flow up to this mass fraction.

We present now our results for the other two geometries (see Fig. 1 (b) and (c)): Figs. 5 and 6 present the results of the effective area for the disc valves with jet angles 0 and 90 degrees, respectively. The measurement results reveal that the effective area is proportional to the relative lift and increases as the valve lift increases for all applied water ratios, including the case of the pure airflow. However, the disc valve with deflection angle $\theta = 0°$ shows higher values than the reaction-like valve $\theta = 90°$ whereas the effective area tendency of disc valves is opposite to its counterpart of the poppet valve.

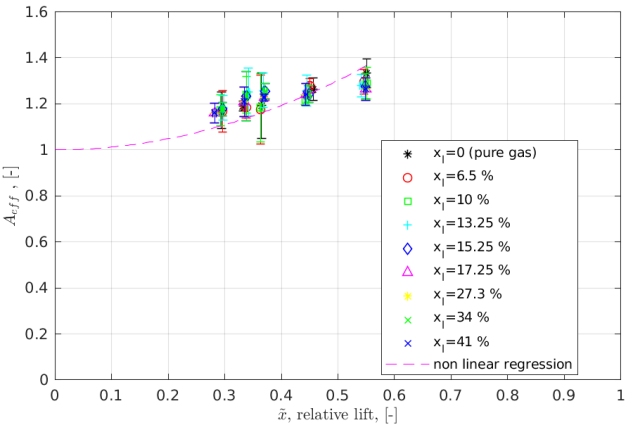

Fig. 5 Effective area vs. relative lift of disc valve $\theta = 0°$

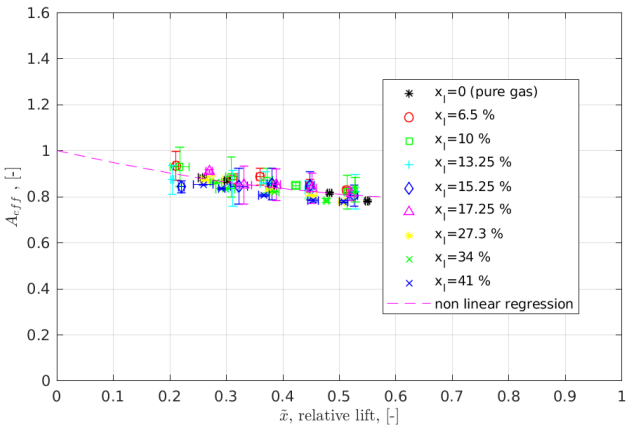

Fig. 4 Effective area vs. relative lift of poppet valve $\theta = 120°$

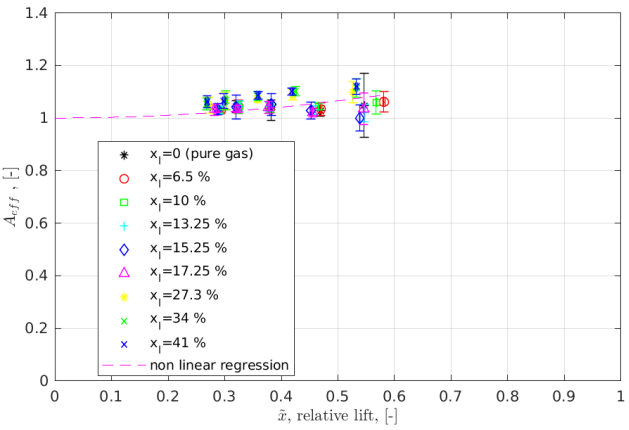

Fig. 6 Effective area vs. relative lift of disc valve $\theta = 90°$

Similarly to the cone valve, the water quality has no significant impact on the effective area (fluid force) values, and its contribution to the overall force is less significant within the investigated range. Finally, the A_{eff} trend differs between 1 up to 1.4 and 1 up to 1.2 regarding the geometries of the valve disc, which are depicted in Figs. 5 and 6, respectively.

The measured data regarding the effective area term for all examined geometries of the safety valve confirm that the influence of the water quality plays a minor role and is negligible. Hence, to provide a model and to supply an estimated standard to predict the relationship between the independent variables and the response variable (dependent), all measured data points in our work were fitted with a single equation, that is, a non-linear curve fitting. The best-fit model for the disc valves follows a parabola equation as:

$$A_{eff} = 1 + a\tilde{x}^2, \tag{13}$$

while the cone valve curve obeys to a polynomial of a second degree

$$A_{eff} = a\tilde{x}^2 + b\tilde{x} + 1. \tag{14}$$

The regression parameters of the effective area with the relative error of the estimated model for three geometries are reported in Table 2.

5.2 Discharge coefficient

The second important factor in sizing the safety valve is the discharge coefficient. We follow the same strategy in analyzing the measured data points in the previous subsection for the examined geometries of the safety valve.

Fig. 7 depicts the relationship between the discharge coefficient and the relative lift of the cone valve. Apparently, the correction factor (discharge coefficient) C_d shows the same tendency as in for the conical valve: the result coincide (within error bounds) with the trend of the pure-air case. Also, the C_d coefficient is reversely proportional to the relative lift; as the opening position increases, the discharge coefficient declines to start from 0.8 falling to 0.58 at a relative lift $\tilde{x} = 0.4$. Beyond this value, the discharge coefficient remains stabilized at approx. 0.55.

Table 2 Regression parameters for A_{eff} and C_d and relative error

valve type, θ	a	b	c	d	max. error A_{eff} %	max. error C_d %
120°	0.373	−0.563	1.566	−1.678	11.9	11.9
0°	1.207	-	-0.593	-	15.8	4.0
90°	0.261	-	-0.452	-	10.9	6.5

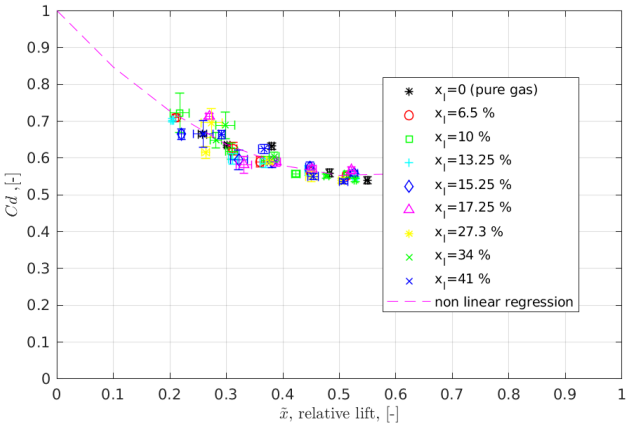

Fig. 7 Discharge coefficient vs. relative lift of poppet valve $\theta = 120°$

Compared to the conical valve, the discharge coefficient for a disc valve shows higher values with the same tendency, declining against the relative valve rising, see Figs. 8 and 9. The reaction-like valve (θ = 90°, Fig. 9) gives higher discharge coefficients, e.g. 0.72 at 0.55 relative valve lift, compared to the value of 0.55 of the purely reversed one ($\theta = 0°$, Fig. 8).

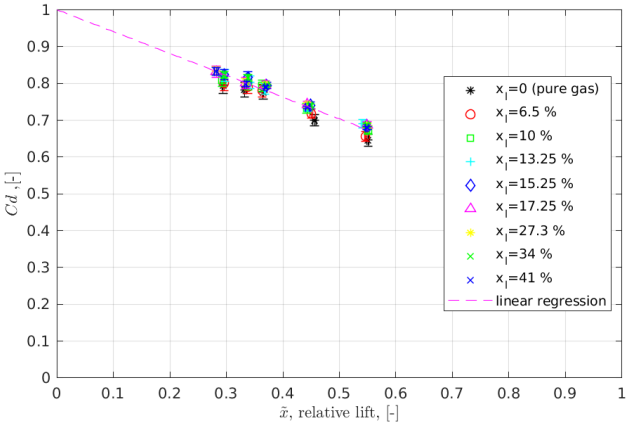

Fig. 8 Discharge coefficient vs. relative lift of disc valve $\theta = 0°$

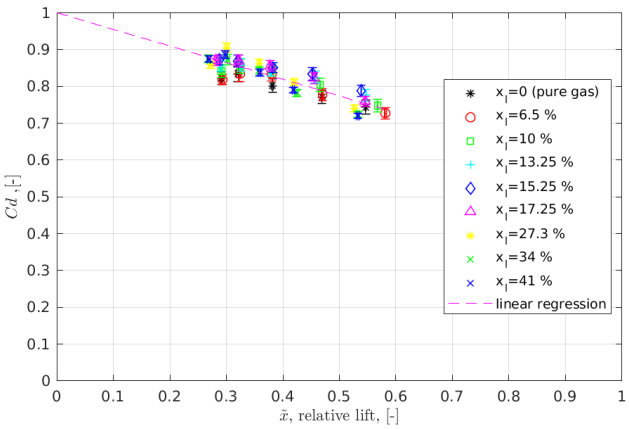

Fig. 9 Discharge coefficient vs. relative lift of disc valve $\theta = 90°$

We also provide a polynomial fit for the discharge coefficients to ease the use. For the poppet valve, we assume

$$C_d = c\tilde{x}^2 + d\tilde{x} + 1, \tag{15}$$

while, for the disc valves, we propose a linear function:

$$C_d = 1 + c\tilde{x}. \tag{16}$$

The regression parameters of the effective area – Eqs. (13) and (14) and the discharge coefficient – Eqs. (15) and (16) – with the relative error of the proposed model are given in Table 2.

Our results of the discharge coefficients for three geometries are compatible with the literature. Focused on the effect of pressure ratio, Boccardi et al. [24] reported $C_d \approx 0.73$ at 5 bar(a) in the case of steam flow. Moreover, they observed that the vapour quality effect is less pronounced (see Fig. 7 in [24]). Schmidt and Egan in [7] report values around C_d = 0.73–0.78 for steam/water mixture for a wide range of commercial safety valves. Finally, Scuro et al. [28] address higher values of discharge coefficient C_d = 0.975–0.773 in the case of dry steam saturated revised by IAPWS-IF97 as a function of extensive disc lift range up to 18 mm.

6 Conclusion

This work unveiled the effect of mixture mass fraction on the flow force and flow performance of safety valves in terms of effective area and discharge coefficient. The influence of the injected water ratios has been presented by studying the change in the momentum force and its effects on the valve disc for three geometries of a safety valve. We employed the DIER's omega technique to predict the theoretical mass flow rate and hence extracting the discharge coefficient of the flow in the case of the frozen mixture.

Through the experiments, we have shown that the mass fraction plays a minor role in the overall force (up to approx. 40 % mass fraction), which is consistent with the corresponding literature [15, 27, 29]. We have highlighted these effects by comparing the effective area of three different geometries of the safety valve. In the case of the poppet (conical) valve, the fluid force decreases with increasing the valve lift, while for disc valves, the fluid force increases with the increase of the valve lifts. The effect of increasing mass fraction ratios can be combined into a single quadratic correlation model, as given in Table 2. The discharge coefficients show the same tendencies for the tested geometries; decreasing values with the lift increasing and, even in the multiphase region, do not change significantly, allowing one single correlation to be used over a wide range of mass fractions given in Table 2. This result gives a reasonable estimation for the required discharge factor in the process of valve sizing in the case of two-phase flow for reduced-order modelling.

Our further plan is to extend the range of the valve lift up to 1, i.e. fully open position. We are also planning to build a water-based test rig allowing us to measure the behaviour of water-dominated mixtures.

Acknowledgements

The research reported in this paper was supported by the Higher Education Excellence Program of the Ministry of Human Capacities in the frame of Water Science & Disaster Prevention research area of Budapest University of Technology and Economics (BME FIKP-VIZ).

References

[1] International Organization for Standardization "ISO 4126-1:2013 Safety devices for protection against excessive pressure — Part 1: Safety valves", International Organization for Standardization, Geneva, Switzerland, 2013.

[2] Bazsó, C., Hős, C. "On the Static Instability of Liquid Poppet Valves", Periodica Polytechnica Mechanical Engineering, 59(1), pp. 1–7, 2015. https://doi.org/10.3311/PPme.7049

[3] Wéber, R., Hős, C. "Experimental and Numerical Analysis of Hydraulic Transients in the Presence of Air Valve", Periodica Polytechnica Mechanical Engineering, 62(1), pp. 1–9, 2018. https://doi.org/10.3311/PPme.10336

[4] Bazsó, C., Hős, C. J. "An experimental study on the stability of a direct spring loaded poppet relief valve", Journal of Fluids and Structures, 42, pp. 456–465, 2013. https://doi.org/10.1016/j.jfluidstructs.2013.08.008

[5] Kovács, L., Váradi, S. "Two-phase Flow in the Vertical Pipeline of Air Lift", Periodica Polytechnica Mechanical Engineering, 43(1), pp. 3–18, 1999. https://pp.bme.hu/me/article/view/1454

[6] Darby, R., Meiller, P. R., Stockton, J. R. "Select the Best Model for Two-Phase Relief Sizing", Chemical Engineering Progress, 97(5), pp. 56–65, 2001.

[7] Schmidt, J., Egan, S. "Case Studies of Sizing Pressure Relief Valves for Two-Phase Flow", Chemical Engineering & Technology, 32(2), Special Issue: Chemical Safety, pp. 263–272, 2009. https://doi.org/10.1002/ceat.200800572

[8] Schmidt, J. "Sizing of nozzles, venturis, orifices, control and safety valves for initially sub-cooled gas/liquid two-phase flow – The HNE-DS method", Forschung im Ingenieurwesen, 71(1), Article numer: 47, 2007. https://doi.org/10.1007/s10010-006-0043-3

[9] Kasai, K. "On the Stability of a Poppet Valve with an Elastic Support: 1st Report, Considering the Effect of the Inlet Piping System", Bulletin of JSME, 11(48), pp. 1068–1083, 1968. https://doi.org/10.1299/jsme1958.11.1068

[10] Singh, A. "On the stability of a coupled safety valve-piping system", In: 2nd International Topical Meeting on Nuclear Reactor Thermal Hydraulics (ANS), Santa Barbara, CA, USA, 1983, pp. 929–937.

[11] Singh, A. "An analytical study of the dynamics and stability of a spring loaded safety valve", Nuclear Engineering and Design, 72(2), pp. 197–204, 1982. https://doi.org/10.1016/0029-5493(82)90215-1

[12] Hős, C. J., Champneys, A. R., Paul, K., McNeely, M. "Dynamic behaviour of direct spring loaded pressure relief valves connected to inlet piping: IV review and recommendations", Journal of Loss Prevention in the Process Industries, 48, pp. 270–288, 2017. https://doi.org/10.1016/J.JLP.2017.04.005

[13] Hős, C. J., Champneys, A. R., Paul, K., McNeely, M. "Dynamic behavior of direct spring loaded pressure relief valves in gas service: Model development, measurements and instability mechanisms", Journal of Loss Prevention in the Process Industries, 31, pp. 70–81, 2014. https://doi.org/10.1016/J.JLP.2014.06.005

[14] Darby, R. "The dynamic response of pressure relief valves in vapor or gas service, part I: Mathematical model", Journal of Loss Prevention in the Process Industries, 26(6), pp. 1262–1268, 2013. https://doi.org/10.1016/J.JLP.2013.07.004

[15] Narabayashi, T., Nagasaka, H., Niwano, M., Ohtsuki, Y. "Safety Relief Valve Performance for Two-Phase Flow", Journal of Nuclear Science and Technology, 23(3), pp. 197–213, 1986. https://doi.org/10.1080/18811248.1986.9734973

[16] van Lookeren Campagne, C., Nicodemus, R., de Bruin, G. J., Lohse, D. "A Method for Pressure Calculations in Ball Valves Containing Bubbles", Journal of Fluids Engineering, 124(3), pp. 765–771, 2002. https://doi.org/10.1115/1.1486220

[17] Ng, K. C., Yap, C. "An investigation of pressure transients in pipelines with two-phase bubbly flow", International Journal for Numerical Methods in Fluids, 9(10), pp. 1207–1219, 1989. https://doi.org/10.1002/fld.1650091004

[18] Alimonti, C., Falcone, G., Bello, O. "Two-phase flow characteristics in multiple orifice valves", Experimental Thermal and Fluid Science, 34(8), pp. 1324–1333, 2010. https://doi.org/10.1016/J.EXPTHERMFLUSCI.2010.06.004

[19] Kim, D. K., Min, H. E., Kong, I. M., Lee, M. K., Lee, C. H., Kim, M. S., Song, H. H. "Parametric study on interaction of blower and back pressure control valve for a 80-kW class PEM fuel cell vehicle", International Journal of Hydrogen Energy, 41(39), pp. 17595–17615, 2016. https://doi.org/10.1016/J.IJHYDENE.2016.07.218

[20] Leung, J. C. "A Generalized Correlation for One-component Homogeneous Equilibrium Flashing Choked Flow", AIChE Journal, 32(10), pp. 1743–1746, 1986. https://doi.org/10.1002/aic.690321019

[21] Leung, J. C., Grolmes, M. A. "A Generalized Correlation for Flashing Choked Flow of Initially Subcooled Liquid", AIChE Journal, 34(4), pp. 688–691, 1988. https://doi.org/10.1002/aic.690340421

[22] Leung, J. C., Epstein, M. "A Generalized Correlation for Two-Phase Nonflashing Homogeneous Choked Flow", Journal of Heat Transfer, 112(2), pp. 528–530, 1990. https://doi.org/10.1115/1.2910419

[23] Leung, J C. "Similarity between Flashing and Nonflashing Two-Phase Flows", AIChE Journal, 36(5), pp. 797–800, 1990. https://doi.org/10.1002/aic.690360520

[24] Boccardi, G., Bubbico, R., Celata, G. P., Mazzarotta, B. "Two-phase flow through pressure safety valves. Experimental investigation and model prediction", Chemical Engineering Science, 60(19), pp. 5284–5293, 2005. https://doi.org/10.1016/j.ces.2005.04.032

[25] Darby, R. "Properly Size Safety Relief Systems for any Conditions", Chemical Engineering, 112(9), pp. 42–50, 2005.

[26] Burhani, M. G., Hős, C. "An Experimental and Numerical Analysis on the Dynamical Behavior of a Safety Valve in the Case of Two-phase Non-flashing Flow", Periodica Polytechnica Chemical Engineering, 65(2), pp. 251–260, 2021. https://doi.org/10.3311/PPch.16262

[27] Burhani, M. G., Hős, C. "Estimating the opening time of a direct spring operated pressure relief valve in the case of multiphase flow of fixed mass fraction in the absence of piping", Journal of Loss Prevention in the Process Industries, 66, Article number: 104169, 2020. https://doi.org/10.1016/j.jlp.2020.104169

[28] Scuro, N. L., Angelo, E., Angelo, G., Andrade, D. A. "A CFD analysis of the flow dynamics of a directly-operated safety relief valve", Nuclear Engineering and Design, 328, pp. 321–332, 2018. https://doi.org/10.1016/j.nucengdes.2018.01.024

[29] Dempster, W., Alshaikh, M. "An Investigation of the Two Phase Flow and Force Characteristics of a Safety Valve", Procedia Engineering, 130, pp. 77–86, 2015. https://doi.org/10.1016/J.PROENG.2015.12.177

[30] Arnulfo, G., Bertani, C., De Salve, M. "Prediction of two-phase choked-flow through safety valves", In: 31st UIT (Italian Union of Thermo-fluid-dynamics) Heat Transfer Conference, Como, Italy, 2013, Article number: 012016. https://doi.org/10.1088/1742-6596/501/1/012016

[31] Dempster, W., Elmayyah, W. "Two phase discharge flow prediction in safety valves", International Journal of Pressure Vessels and Piping, 110, pp. 61–65, 2013. https://doi.org/10.1016/j.ijpvp.2013.04.023

[32] Elmayyah, W., Dempster, W. "Prediction of two-phase flow through a safety relief valve", Proceedings of the Institution of Mechanical Engineers, Part E: Journal of Process Mechanical Engineering, 227(1), pp. 42–55, 2013. https://doi.org/10.1177/0954408912453407

[33] Hellemans, M. "The Safety Relief Valve Handbook: Design and Use of Process Safety Valves to ASME and International Codes and Standards", Butterworth-Heinemann Ltd., Oxford, UK, 2010. https://doi.org/10.1016/C2009-0-20219-4

[34] Munson, B. R. "WileyPLUS Blackboard Card for Fundamentals of Fluid Mechanics", Wiley-Blackwell, Hoboken, NJ, USA, 2012.